A FAST BACK-PROJECTION ALGORITHM FOR BISTATIC SAR IMAGING

*Yu Ding and David C. Munson, Jr.**

Coordinated Science Laboratory and
Department of Electrical and Computer Engineering
University of Illinois at Urbana-Champaign
1308 West Main Street, Urbana, IL 61801

ABSTRACT

Using a far-field model, bistatic synthetic aperture radar (SAR) acquires Fourier data on a rather unusual, non-Cartesian grid in the Fourier domain. Previous image formation algorithms were mainly based on direct Fourier reconstruction to take advantage of the FFT, but the irregular coverage of the available Fourier domain data and the 2-D interpolation in the Fourier domain may adversely affect the accuracy of image reconstruction. Back-projection techniques avoid Fourier-domain interpolation, but ordinarily have huge computational cost. In this paper, we present a fast back-projection algorithm for bistatic SAR imaging, motivated by a fast back-projection algorithm recently proposed for tomography. It has reduced computational cost, on the same order as that of direct Fourier reconstruction. Furthermore, this approach can be used for near-field imaging. Simulation results verify performance of this new algorithm.

1. INTRODUCTION

In bistatic SAR imaging, the transmitting and receiving antennas are spatially separated and may move along different paths, whereas in monostatic SAR, a single antenna or colocated antennas are used. Although monostatic SAR imaging is predominant, bistatic SAR geometry is especially useful for certain circumstances. For example, a high powered transmitter can be operated at a safe distance from a target area while a covert receiver is flown close to the scene, collecting returned signals and forming high resolution imagery.

Bistatic SAR imaging is somewhat more involved than the monostatic case, due to the changing bistatic SAR geometry. To achieve computational efficiency, direct Fourier reconstruction (DFR), based on the FFT, has been used for bistatic SAR imaging [1, 2, 3]. In [1, 2], the FFT based method used the far-field approximation for bistatic SAR, and the resulting algorithm has similarity to that in the monostatic case [4]. This method does not consider effects of wavefront curvature. Soumekh proposed a wavenumber domain algorithm accounting for wavefront curvature effects [3], which is similar to the $\omega - k$ algorithm for monostatic SAR. But, this approach involves challenging interpolation in the 2-D Fourier domain that may cause artifacts in the image domain. It also has the disadvantage of data coverage in a region of irregular shape in the 2-D Fourier domain, which makes it somewhat difficult to utilize all the data during reconstruction.

The standard back-projection (BP) algorithm can eliminate the above problems, but it has huge computational cost. For an $N \times N$ image, the cost of BP is $O(N^3)$, whereas the cost of direct Fourier reconstruction (DFR) is $O(N^2 log_2 N)$, ignoring the interpolation. In this paper, we develop a fast BP algorithm for bistatic SAR, motivated by the fast BP algorithm proposed for tomography [5]. It achieves computational cost on the same order as that of the DFR.

In Section II we establish the bistatic SAR imaging model. Then we illustrate the connection between the standard BP algorithm and the benchmark wavenumber domain ($\omega - k$) algorithm for bistatic SAR in Section III. The fast BP algorithm for tomography is briefly reviewed in Section IV. In Section V, we outline the fast BP algorithm for bistatic SAR. Finally we give simulation results to validate our approach in Section VI.

2. BISTATIC SAR IMAGING MODEL

Figure 1 shows a typical bistatic SAR geometry, where both the transmitting and receiving antennas move along straight paths. We define the cross-range direction x to be the same as the direction of the receiver flight path, and the range direction y to be perpendicular to the cross-range direction. The closest distance from the receiver to the center of the ground patch is y_c. At the times of pulse transmission, the positions of the transmitting and receiving antennas are evenly spaced along their paths. The angular separation be-

*This research was supported by DARPA and administered by AFOSR under contract F49620-98-1-0498.

tween the transmitter and the receiver with respect to the center of the ground patch is called the *bistatic angle*, and the line that evenly divides the bistatic angle is called the *bisector*. At each position (x_t, y_t), the transmitting antenna sends a microwave pulse. The receiving antenna at position (x_r, y_c) records the return signal from the scene lying within the radar footprint. The round-trip distance from the transmitter to a point reflector at (x', y') and then back to the receiver is

$$R(x_t, y_t, x_r; x', y') = \sqrt{(x_t - x')^2 + (y_t - y')^2} + \sqrt{(x_r - x')^2 + (y_c - y')^2}. \quad (1)$$

Both radars work in spotlight mode, i.e., both antennas are steered at the same ground patch during the entire operation period.

The typical microwave pulse sent by the transmitting antenna is a linear FM chirp signal of the form $Re\{s(\tau)\}$, where

$$s(\tau) = p(\tau) \cdot e^{j(\omega_0 \tau - \pi\alpha\tau^2)} \quad (2)$$

with

$$p(\tau) = \begin{cases} 1 & \text{if } |\tau| \le \frac{T}{2} \\ 0 & \text{otherwise.} \end{cases} \quad (3)$$

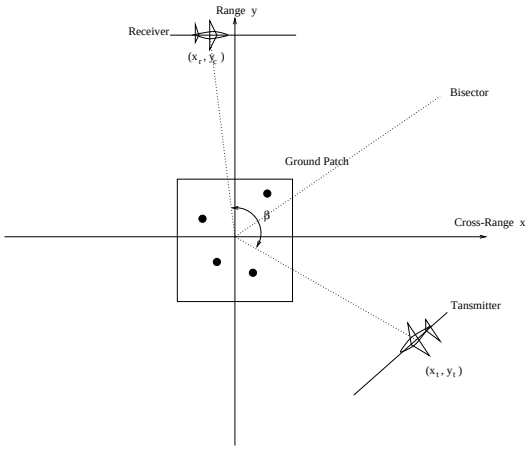

Fig. 1. Bistatic SAR Imaging Model.

The radar return from a unit point reflector at (x', y') is a delayed version of the above transmitted signal, with delay $\Delta_\tau = R(x_t, y_t, x_r; x', y')/c$. The return signal can be expressed as:

$$h(x_t, y_t, x_r, \tau; x', y') = \cos(\omega_0(\tau - \Delta_\tau) - \pi\alpha(\tau - \Delta_\tau)^2). \quad (4)$$

Note that x_t and y_t both can be expressed as functions of x_r, when the two antenna trajectories are given. In the following we will express the returned signal as well as other related parameters as functions of x_r and τ only.

The returned signal is the superposition of the returns from all reflectors within the radar footprint. After demodulation and phase compensation, the returned signal can be shown to be

$$d(x_r, \omega) = \iint g(x', y') \cdot exp(-j\frac{\omega}{c} R(x_r; x', y'))\, dx'\, dy', \quad (5)$$

where

$$\omega = \omega_0 - 2\pi\alpha(\tau - \frac{R_0(x_r; x', y')}{c}) \quad (6)$$

on the interval $-\frac{T}{2} + \frac{R_{max}}{c} \le \tau \le \frac{T}{2} + \frac{R_{min}}{c}$, where T is the transmitted chirp pulse length. $g(x', y')$ is the scene reflectivity at (x', y'). R_{max} and R_{min} are the longest and shortest distances from the transmitter to the ground patch and then back to the receiver, for each pair of the transmitter-receiver positions. R_0 is the distance from the transmitter to the center of the scene and back to the receiver. In a typical bistatic SAR setting, the range of ω can be well approximated by $\omega_0 - \pi\alpha T \le \omega \le \omega_0 + \pi\alpha T$.

The demodulated SAR data becomes the 1-D Fourier transform of the projections of the ground patch reflectivity $g(x', y')$ along ellipses, with the two antennas at the foci [2].

3. STANDARD BACKPROJECTION ALGORITHM AND WAVENUMBER DOMAIN ALGORITHM

Back-projection is the adjoint operation of projection. It reconstructs the image by smearing or back-projecting the projections along the original paths of integration. Let

$$b(x_r, l) = \int_\omega d(x_r, \omega) \cdot exp(-j\omega l) d\omega \quad (7)$$

be the signal before back-projection. Then the image can be reconstructed as the back-projection of $b(x_r, l)$ along elliptical paths:

$$\hat{g}(x, y) = \sum_{i=1}^{P} b(x_{ri}, (\sqrt{(x_{ti} - x')^2 + (y_{ti} - y')^2} + \sqrt{(x_{ri} - x')^2 + (y_c - y')^2})/c) \Delta x_{ri}, \quad (8)$$

where P is the total number of projections, i.e., the total number of sampling points in coordinate x_r.

Before developing the fast back-projection algorithm for bistatic SAR, we first point out the connection between the standard BP algorithm and the benchmark wavenumber domain ($\omega - k$) algorithm in the bistatic case. One can begin from the development of the $\omega - k$ algorithm for bistatic SAR [3], which states that the collected SAR raw data, after Fourier transformation in the azimuth direction x_r, is the 2-D Fourier transformation of the scene reflectivity $g(x', y')$, distributed along certain trajectories in the 2-D Fourier domain. Then by using the 2-D inverse Fourier transform

with a change of variables (interpolation), it can be shown that, alternatively, the same scene reflectivity can be reconstructed by back-projecting the scene projections along their original elliptical paths, with the transmitting and receiving antennas at the foci of the ellipses.

4. FAST BACK-PROJECTION ALGORITHM IN TOMOGRAPHY

Basu and Bresler proposed a fast BP algorithm in [5], which is an accelerated version of the standard BP reconstruction used in tomography. It reduces the computational cost from $O(N^3)$ to $O(N^2 log_2 N)$, for an $N \times N$ image. The central idea of this fast algorithm is rooted in the angular band-limited property, or the so-called bow-tie approximation, of the Radon transform of an image, i.e., images that are half the size of the original image can be reconstructed from half the number of the projections. So, for example, given N projections for a $N \times N$ image, if we use the standard BP algorithm, then we need to back-project N projections for each of the N^2 pixels, and the total computational cost is N^3. If we divide the image into four subimages each with size $N/2 \times N/2$, then using the bow-tie property, we only need to back-project $N/2$ projections for each pixel, and the computational cost for each subimage is $N^3/8$, and the total cost is $N^3/2$. So by dividing the original image into four subimages, we reduce the computation by a factor of two. By recursively decomposing the image by a factor of 2 and back-projecting using half the number of projections for smaller subimages, the $O(N^2 log_2 N)$ computational cost can be achieved.

A holdoff factor was introduced in this fast algorithm to manage the tradeoff between computational cost and the accuracy of the reconstruction. A holdoff factor of n indicates that we use the full set of projections for back-projection in the first n decompositions of the image.

5. FAST BACK-PROJECTION ALGORITHM FOR BISTATIC SAR IMAGING

A close connection between SAR and tomography was shown in [4], which presented a filtered back-projection algorithm for monostatic spotlight mode SAR imaging. A fast back-projection algorithm for monostatic spotlight mode SAR imaging recently has been proposed in [6], motivated by the fast back-projection algorithm in tomography [5]. Here we investigate the feasibility of a fast back-projection algorithm for bistatic SAR image formation, using the similar idea of recursively decomposing the image by a factor of 2 and back-projecting half the number of projections to form subimages.

To develop a fast BP algorithm for bistatic SAR, we first must establish the validity of the angular band-limited property associated with the bistatic case. This point can be addressed by recalling that in the far-field bistatic approximation, the dechirped SAR data corresponding to each pair of transmitter-receiver positions can be approximated as a slice of the 2-D Fourier transform of the ground reflectivity. The orientation of the slice is that of the bisector corresponding to the pair of the transmitter-receiver positions, and the bandwidth is that of the transmitting pulse scaled by $\frac{2}{c}\cos\frac{\beta}{2}$, where β is the bistatic angle [1, 2]. So, according to Nyquist, the necessary spacing between slices in the 2-D Fourier domain is inversely proportional to the ground patch size, which means that we can use proportionately fewer projections for the reconstruction of a smaller ground patch. Thus, the idea underlying the fast back-projection algorithm holds.

There are several major differences between the fast BP algorithm for tomography and our fast BP algorithm for bistatic SAR: First, the back-projection is performed along elliptical paths with foci at the two antenna positions, instead of along a straight path. Second, the SAR data are frequency-offset with center frequency $\frac{\omega_0}{c}$, and all the SAR data are within a region of limited angular coverage of perhaps a few degrees. Thus, the interpolation in the radial direction becomes bandpass interpolation. In standard tomography, all the projections are low-pass signals, with 360 degree angular coverage. Also our interpolations in the x_r and l directions are complex-valued due to the fact that radar reflectivity is a complex quantity. The recursive fast BP algorithm for bistatic SAR is as follows.

1. Obtain projections $b(x_r, l)$ according to Eqn. (7).
2. Modulate $b(x_r, l)$ to its low-pass version, by multiplying by $e^{j\frac{\omega_0}{c}l}$.
3. Subdivide the image into four subimages.
4. Shift and truncate the projections for each subimage.
5. Radially interpolate $b(x_r, l)$, then modulate by $e^{-j\frac{\omega_0}{c}l}$.
6. Decimate $b(x_r, l)$ in the x_r direction to form a half-sized projection set for each of the four subimages.
7. Back-project using Eqn. (8) if in the last step of recursion. Otherwise, modulate the projections to their lowpass versions and go to Step 3.

6. SIMULATION RESULTS

In this section, we present simulation results for bistatic SAR imaging using the fast algorithm. The bistatic geometry is shown in Fig. 2. In our simulations, we assume that the cross-range direction is parallel to the flight path of the receiver, and the flight path of the transmitter is parallel to the range direction. There are four unit point targets in

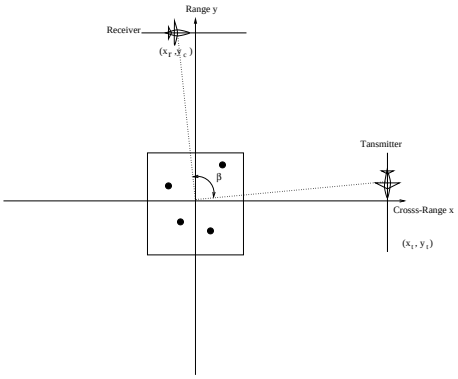

Fig. 2. Bistatic SAR imaging scenario.

the scene, with pixel positions (96,62), (156,102), (56,202) and (216,182), where the upper left corner is (0,0). The parameters are: Carrier frequency = 10GHz; Bandwidth = 500MHz; Radar flight paths straight with middle positions at (0,y_0) and (y_0,0), respectively, where y_0 is the nearest distance from the transmitter to the center of the ground patch. The antenna positions are evenly spaced for both the transmitter and the receiver. The ground patch size is 256×256. The raw data set is 512×512, with one dimension corresponding to slant range from transmitter to ground patch to receiver, and the other dimension corresponding to the cross-range positions of the receiver. The range of viewing angles α of the receiver is 3^o. The bistatic angle β is about 90^o during the data collection. The closest distance between the flight paths and the center of the ground patch are both 10 times the ground patch size, which is a moderate near-field scenario.

We first reconstructed an image using the standard (slow) implementation of the elliptical back-projection method. The four point targets are faithfully reproduced at their correct positions, as shown in Fig. 3(a). The total CPU time was 402 seconds. Then we applied the fast algorithm with hold-off factor set to 1. The CPU time was 59 seconds. The reconstruction is shown in Fig. 3(b), which is virtually identical to that shown in Fig. 3(a). Our experiments showed that when the image size was smaller that 8×8, there was no gain in speed for the fast algorithm. Thus, we terminated the iteration in the fast algorithm when the size of the subimages reached 8×8. For images with size larger that 256×256, the speed-up factor will increase, according to $N/logN$.

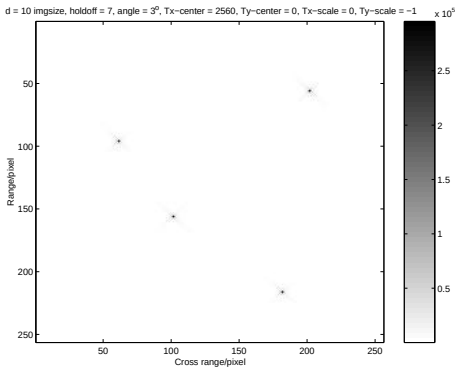

(a)

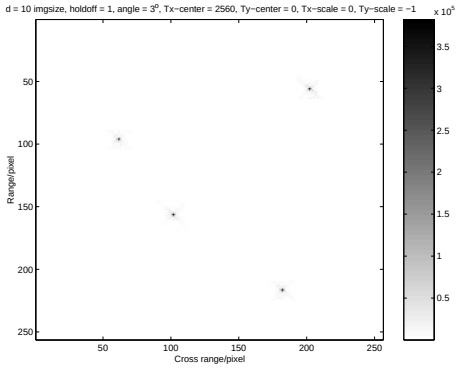

(b)

Fig. 3. Bistatic SAR imaging using standard and fast elliptical back-projection.

7. REFERENCES

[1] Dean L. Mensa, *High Resolution Radar Imaging*, Artech House, Dedham, MA, 1981, pp.142-150.

[2] O. Arikan and D. C. Munson, Jr., "A tomographic formulation of bistatic synthetic aperture radar," in *Proc. of the ComCon 88, Advances in Communication sand Control Systems*, Baton Rouge, LA, Oct. 1988.

[3] M. Soumekh, "Bistatic synthetic aperture radar inversion with application in dynamic object imaging," *IEEE Trans. on Signal Processing*, vol. 39, pp. 2044–2055, Sept. 1991.

[4] D. C. Munson, Jr., J. D. O'Brien, and W. K. Jenkins, "A tomographic formulation of spotlight-mode synthetic aperture radar," *Proc. of the IEEE*, vol. 71, pp. 917–925, Aug. 1983.

[5] S. Basu and Y. Bresler, "$O(N^2 log_2 N)$ filtered backprojection reconstruction algorithm for tomography," *IEEE Trans. on Image Processing*, vol. 9, pp. 1760–1773, Oct. 2000.

[6] S Xiao, D. C. Munson, Jr., S. Basu, and Y. Bresler, "An $N^2 logN$ back-projection algorithm for SAR image formation," in *Proc. of 34th Asilomar Conf. on Signals, Systems and Computers*, Pacific Grove, CA, Nov. 2000, pp. 3–7.